Int J Adv Manuf Technol (2011) 56:841–855
DOI 10.1007/s00170-011-3231-8

ORIGINAL ARTICLE

Prediction of chip flow angle to study the relation between chip flow and ratio of the cutting edge lengths using sharp corner tools

Qingming Wang · Hailong Lin · Zhenfeng Zhang

Received: 20 October 2010 / Accepted: 9 February 2011 / Published online: 1 March 2011

Abstract Chip flow control is an important issue for automated machining. Using the cutting power equilibrium equation of Usui et al. (ASME J Eng Ind 100:222–228, 1978) and Usui and Hirota (ASME J Eng Ind 100:229–235, 1978), a new chip flow angle prediction model is derived for helical vee grooves turning with sharp corner tools and is expressed as the transformed cutting power equilibrium equation in which the value of the principal cutting force F is experimentally measured. In this study, RATIO is defined as the ratio of the main to the minor cutting edge length engaged in cutting and is a set variable on the basis of the constant equivalent cutting area. The chip flow angle corresponding to different values of RATIO predicted by the current model shows good correlation with the experimental measurement, and FEM simulation results for various cutting conditions. An investigation of the effect of RATIO on the chip flow angle is made under various cutting conditions, and it is demonstrated that RATIO has a significant influence on the chip flow angle.

Keywords Chip flow angle · Cutting edge length · Sharp corner tools · Vee grooves turning

1 Introduction

A complicated interaction of plastic and elastic deformations happens in the shear zone which determines the geometry and motion of the chip during chip formation. Chip control, which depends heavily on the nature of the chip flow and its direction on the rake face of the cutting tools, will improve the quality of the workpiece, prolong the life of tools and machines, and optimize the geometry of tool [1–3]. The direction of chip flow in metal machining as well as continuous mode operation is important for chip control and has long been recognized and re-emphasized recently [1].

Obviously, the chip control is closely related to the chip flow angle. In the recent 50 years, many useful models on chip flow in 3-D cutting process have been developed in scientific research. Stabler [4] purposed that the chip flow angle was equal to the inclination angle in oblique cutting regardless of cutting parameters. Later, he [5] also postulated the revised flow rule that the chip flow angle was proportional to the inclination angle with the proportionality factor varying between 0.9 and 1 depending on the workpiece material and cutting conditions. However, Stabler's models are only satisfied well by using a cutting tool with only one straight cutting edge. In many practical machining operations, cutting tools with major and minor cutting edges are engaging with the workpiece. The prediction model in our study is satisfied well in double-edge cutting case. In a subsequent study, Armarego and Brown [6] evaluated Stabler's flow rule experimentally for a wide range of inclination angles and rake angles and concluded that Stabler's flow rule was only adaptive to some values of rake angles. Colwell [7] suggested a simplified geometrical method, which assumed that the chip flow angle over the tool rake face was approximately perpendicular to the cutting edge chord representing the major axis of the cut, as shown in Fig. 1.

However, the predicted results of the chip flow angle only have satisfactory agreement with the cutting conditions with zero tool inclination and rake angles, regardless of the influence of various workpiece materials. Hu et al.

Q. Wang (✉) · H. Lin · Z. Zhang
East China University of Science and Technology,
Shanghai, People's Republic of China
e-mail: wangqm021@gmail.com

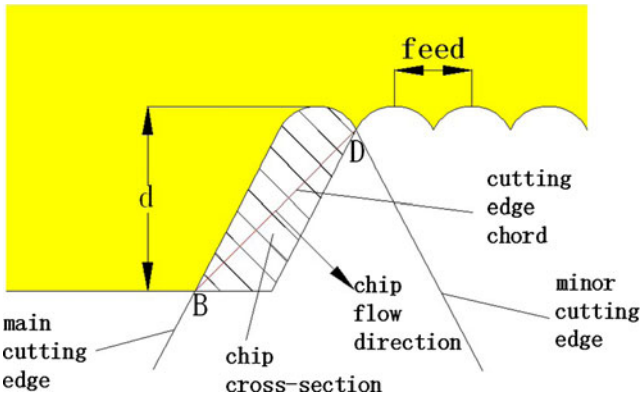

Fig. 1 Scheme of cutting edge chord (top view of the tool, adapted from Bradley and Thomas [31])

[8] generalized Colwell's model to non-zero inclination and rake angles by introducing the concept of an equivalent cutting edge which was defined to be the line joining the end points of the projection of the uncut chip area on the tool rake face. The chip flow angle, with respect to the normal to the equivalent cutting edge in the rake face, was then obtained by applying Stabler's chip flow rule with respect to the equivalent tool geometrical angles corresponding to the equivalent cutting edge. In literature [9, 10], the chip flow angle can also be obtained by other prediction models based on reasonable assumptions.

The energy approach for chip flow angle prediction was originally proposed by Usui et al. [11, 12] who minimized the cutting energy comprised of the shear energy and the friction energy to find the chip flow angle for sharp corner tools having zero side and end cutting edge angles. According to them, the shear plane could be divided into several equivalent shear planes along the active cutting edge. However, in Usui et al.'s model, the significant parameters such as equivalent shear angle, shear stress, and equivalent friction angle which greatly affect chip flow angle prediction in three-dimensional cutting are just generated from orthogonal cutting experiments. Therefore, chip flow angle prediction accuracy will be inevitably affected by approximation. The energy approach was also used by Shamoto and Altintas [13]. They utilized either the maximum shear stress or the minimum energy principle to develop a numerical approach to calculate the chip flow angle in oblique machining.

During the last decade, many novel approaches were proposed to study chip flow angle prediction. Adibi-Sedeh et al. [14–16] proposed a generalized upper-bound model for calculating the chip flow angle in oblique cutting using flat-faced nose radius tools and sharp corner tools that cut along both the side and the end cutting edges. The shear area and friction area were calculated corresponding to the similarity between orthogonal and oblique cutting in the equivalent cutting plane. The chip flow angle was obtained by minimizing the cutting power comprised of shear power and friction power. John S. Strenkowski, Albert J. Shih, and Jong-cherng Lin [17] used a finite model instead of experimental measurement to supply the orthogonal cutting data which consists of the shear angle, the shear stress acting on the shear plane, and the friction angle for the analytical model developed by Usui et al. [11, 12]. However, the cutting data which greatly affect chip flow angle prediction in three-dimensional cutting are still supplied by the orthogonal cutting process simulated by FEM software. Wen DH, Zheng L, Li ZZ, and Hu [18] proposed a model of the chip flow angle calculation for a sharp corner tool considering cutting geometry variations based on the equivalent cutting edge method. The basic depiction of the equivalent cutting edge and chip flow direction is similar to Colwell's model. The chip flow angle η_c can be expressed as follows:

$$\eta_c = k\left\{\kappa_r - \arcsin\left[\frac{a_p(\cot\kappa_r + \cot\kappa_r') - f}{b_{ch}(\cot\kappa_r + \cot\kappa_r')}\right]\right\} \tag{1}$$

where k is a revised factor equal to 0.9~1, κ_r is the main cutting edge angle, κ_r' is the minor cutting edge angle, a_p is the depth of cut, f is the feed rate, b_{ch} is the length of equivalent cutting edge which can be expressed as the following:

$$b_{ch} = \left[\frac{a_p^2}{\sin^2\kappa_r} + \frac{f^2\sin^2\kappa_r}{\sin(k_r + k_r')} + \frac{2a_p f}{\tan(k_r + k_r')}\right]^{1/2} \tag{2}$$

However, the length of equivalent cutting edge b_{ch} is considered to be affected by the feed rate f while in helical vee groove turning the equivalent cutting edge b_{ch} stays constant and the prediction model may not be satisfied well. Wen DH, Zheng L, Li ZZ, and Hu [19] also proposed a new method for predicting the chip flow angle under different cutting parameters using the single-point and nose-radiused cutting tools. The effects of the major cutting edge, minor cutting edge, corner radius, and cutting parameters (depth of cut and feed rate) on the chip flow direction were studied by calculating the components of the thrust cutting force for the major and minor cutting edges based on the hypothesis that the chip flow direction was also the thrust force direction. Zou GP, Yellowley I, and Seethaler RJ [20] proposed a new upper-bound model that incorporated force equilibrium parallel to the cutting edges for single edge oblique cutting operations. In the energy approach, *SLIP* was defined as the ratio of the shear velocity imparted to the chip on the shear plane parallel to the cutting edge, to the incoming velocity in the same direction; *RATIO* was defined as the ratio of the friction force on the rake face to

the resultant shear force in the shear plane. Experimental force data but no shear angle data is needed for the analysis of cutting operations with non-straight cutting edges. However, the new upper-bound model is only satisfied by oblique cutting with single cutting edge. Double-edge cutting is investigated in our study, and we define RATIO as the ratio of the length of the main cutting edge in engagement with the workpiece to the length of the minor cutting edge in engagement with the workpiece. RATIO can be expressed as follows:

$$\text{RATIO} = \frac{\text{Length of the main cutting edge in engagement with the workpiece}}{\text{Length of the minor cutting edge in engagement with the workpiece}}.$$

As the previous work above showed, many researchers have studied the rule of the chip flow angle and proposed various prediction models of chip flow angle validated by experiments and FEM. However, the relationship between the chip flow angle and ratio of the lengths of the cutting edges engaged in cutting has not been studied yet. In this study, to investigate the effect of RATIO on the chip flow angle, the value of RATIO is variable and the equivalent cutting area which is the projection of the area of the rake face involved in cutting on the datum plane is set to be constant under a specific oblique cutting condition.

The minor cutting edge involved in cutting in case of the nose radius is much smaller than the feed rate and the depth of cut. The tool can be taken as a sharp corner tool with zero nose radius in case the lengths of the main and minor cutting edge in engagement with the workpiece are much larger than the nose radius, which is the case in many industrial machining operations such as tapping, threading, and hobbing [21, 22]. In this study, double edges turning with sharp corner tools are analyzed to create a new prediction model for the chip flow angle and study the relation between the chip flow angle and the lengths of the cutting edges. As shown in Fig. 1, the equivalent cutting edge was defined to be the vector (or line) joining the two intersection points of the side cutting edge with the uncut work surface and the end cutting edge with the newly cut spiral work surface in the rake face of the tool [23]. In this research, the feed rate f is larger than the equivalent cutting edge chord |BD|, which is the case of helical vee grooves turning with the two intersection points B and D all on the uncut work surface shown in Fig. 2. The depth of cut d and the main (minor) cutting edge angle Cs (Ce) are adjusted to keep the equivalent cutting area constant and set RATIO variable to study the effect of various values of RATIO on the chip flow angle.

In this research, we define a global coordinate system X–Y–Z to obtain the expression of shear area A_S, friction area A_f, and cutting energy U which consists of the sum of shear power W_S and the friction power W_f. In this study, cutting power equilibrium equation $V \cdot F = W_S + W_f$ [11, 12], in which F is the principal component of cutting force measured from experiments, can be substituted into with the measured principal cutting force F, and the expressions of the shear power W_S and the friction power W_f. Then the transformed equation of cutting power equilibrium with respect to the two main variables, RATIO and the chip flow angle, is obtained as a new chip flow angle prediction model to study the relation between RATIO and the chip flow angle using arbitrarily oriented sharp corner tools that cut along both the main and minor cutting edges.

2 Model setting up

2.1 Description of the configuration of an arbitrarily oriented sharp corner tool

OG is the main cutting edge and OF is the minor cutting edge of the tool as shown in Fig. 3 adapted from Hu et al.

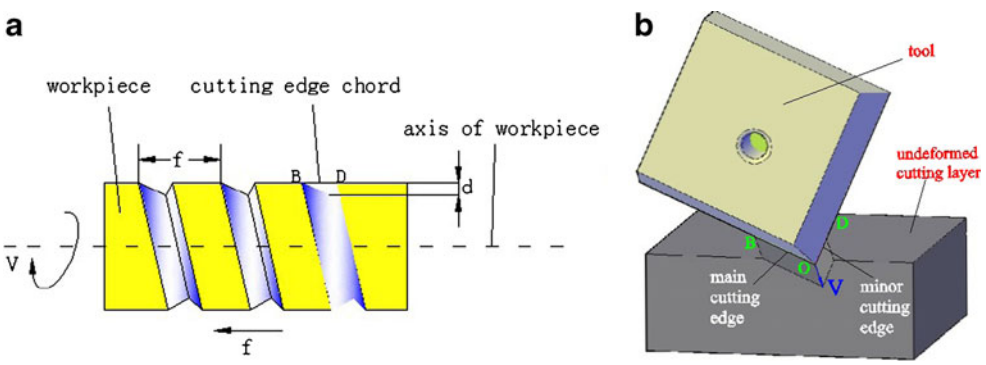

Fig. 2 Scheme of helical vee grooves turning. **a** Top view of the tool. **b** Back view of the tool

[8]. The plane OGCF is the rake face of the tool. |OB| and |OD| are the lengths of the main and the minor cutting edges in engagement with workpiece, respectively.

As shown in Fig. 3, the global coordinate system X–Y–Z is defined as:

The *X*-axis is along the vector **DB** joining the two intersection points on the lines OB and OD;
The *Z*-axis is the vector normal to the rake face of the tool;
The *Y*-axis is found by the right hand rule convention.

OG′ OF′, and GC′ are the normal projection of OG, OF, and GC on the datum plane respectively. The normal rake angle α_n is the angle between the rake face and the datum plane measured perpendicular to the main cutting edge OG; the inclination angle i is the angle between the main cutting edge OG and OG′; the main cutting edge angle C_S is the projection of the angle between OG and the negative *Y*-axis on the datum plane while the minor cutting edge angle C_e is the angle between OF′ with the opposite feed direction; the depth of cut d is the radial interference between the tool and the workpiece.

2.2 Chip formation kinematics and the shear area calculation

The cutting velocity **V** can be expressed in X–Y–Z coordinate system as [14]:

$$\mathbf{V} = \begin{pmatrix} \dfrac{\sin i \tan C_S - \tan \alpha_n}{\sqrt{\cos^2 i \sec^2 C_S + (\tan \alpha_n - \tan C_S \sin i)^2}} \\ \dfrac{-\cos i(\tan C_S \sin \alpha_n + \sin i \cos \alpha_n)}{\sqrt{\cos^2 i \sec^2 C_S + (\tan \alpha_n - \tan C_S \sin i)^2}} \\ \cos i \cos \alpha_n \end{pmatrix} \cdot V$$

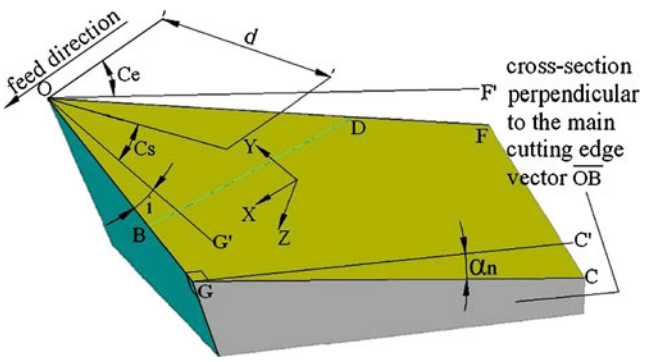

Fig. 3 Geometry of a sharp point tool with a major cutting edge angle C_S, minor cutting edge angle C_e, inclination angle i and normal rake angle α_n (adapted from Hu et al. [8])

The chip velocity $\boldsymbol{V_C}$ can be expressed as:

$$V_C = \begin{pmatrix} -V_C \cos \eta \\ -V_C \sin \eta \\ 0 \end{pmatrix}$$

It should be noted that η is defined to be the angle between the chip velocity $\boldsymbol{V_C}$ and the negative *X*-axis rather than the chip flow angle. V and V_C are the magnitudes of the cutting velocity $\boldsymbol{V}$ and the chip velocity $\boldsymbol{V_C}$ respectively. $\boldsymbol{V_S}$ can be expressed as $\boldsymbol{V_S}=\boldsymbol{V_C}-\boldsymbol{V}$ in the effect plane shown in Fig. 4a. The equivalent cutting area ΔOBD is divided by the line OE along the chip flow direction while the shear surface area ΔOBE′ and ΔODE′ share the common boundary OE′ which is the projection of OE on the shear surface as shown in Fig. 4a, b. The total shear surface area is obtained by summing up the value of the main shear surface area ΔOBE′ and the minor shear surface area ΔODE′ shown in Fig. 4b.

To express concisely, as shown in Fig. 5a, a sharp corner tool with zero rake angle and inclination angles, 10° of the clearance and the end clearance angle and 90° of the tool tip angle is considered in this research. So the line normal to the main cutting edge on the rake face of the symmetric sharp tool is parallel to the minor cutting edge and the chip flow angle equals the angle between the chip flow direction and the minor cutting edge.

For the sharp point tool shown in Fig. 5a, the effect rake angle α_e is zero, the angle between the main and the minor cutting edge is the right angle and the main cutting edge angle C_S equals the minor cutting edge angle C_e. According to the coordinate system shown in Fig. 5b, the relation between the chip flow angle η_c and the angle η can be expressed as $\eta_c = \eta - C_e = \eta - C_S$, and we can simplify the expressions of $\boldsymbol{V}$, $\boldsymbol{V_C}$, and $\boldsymbol{V_S}$ as:

$$\mathrm{V} = \begin{pmatrix} 0 \\ 0 \\ 1 \end{pmatrix} \cdot V$$

$$V_C = \begin{pmatrix} -\cos(\eta_C + C_S) \\ -\sin(\eta_C + C_S) \\ 0 \end{pmatrix} \cdot V_C$$

and

$$V_S = V_C - V = \begin{pmatrix} -V_C \cos(\eta_C + C_S) \\ -V_C \sin(\eta_C + C_S) \\ -V \end{pmatrix},$$

respectively. So the relation between $\boldsymbol{V}$ and $\boldsymbol{V_C}$ can be calculated as $\tan \phi_e = \frac{V_C}{V}$ where Φ_e is the equivalent shear angle in the effect plane.

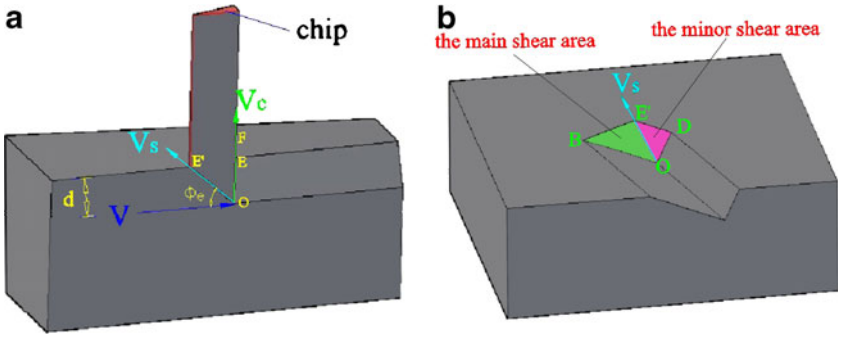

Fig. 4 For the case of zero rake angle. **a** Geometric relationship of V, V_S, and V_C on the effect cutting plane and **b** the total shear area consisting of the main and the minor shear area

In the global coordinate system X–Y–Z shown in Fig. 5b, the points of O, B, D, and E on the rake face of the tool can be expressed as:

$$O : (0,0,0)^T$$

$$B : \frac{d}{\cos Cs} \cdot \begin{pmatrix} \sin Cs \\ -\cos Cs \\ 0 \end{pmatrix}$$

$$D : \frac{d}{\sin Cs} \cdot \begin{pmatrix} -\cos Cs \\ -\sin Cs \\ 0 \end{pmatrix}$$

$$E : \frac{d}{\sin(\eta_C + Cs)} \cdot \begin{pmatrix} -\cos(\eta_C + Cs) \\ -\sin(\eta_C + Cs) \\ 0 \end{pmatrix}$$

In light of the expression of the shear velocity V_S, the point E′ on the shear plane corresponding to the point E on the rake face of the tool can be expressed as:

$$E' : \frac{d}{\sin(\eta_C + Cs)} \cdot \begin{pmatrix} -\cos(\eta_C + Cs) \\ -\sin(\eta_C + Cs) \\ -\frac{V}{V_C} \end{pmatrix}$$

So we can calculate the expressions of the vectors as follows:

$$\mathbf{OB} = \frac{d}{\cos Cs} \cdot \begin{pmatrix} \sin Cs \\ -\cos Cs \\ 0 \end{pmatrix}$$

$$\mathbf{OD} = \frac{d}{\sin Cs} \cdot \begin{pmatrix} -\cos Cs \\ -\sin Cs \\ 0 \end{pmatrix}$$

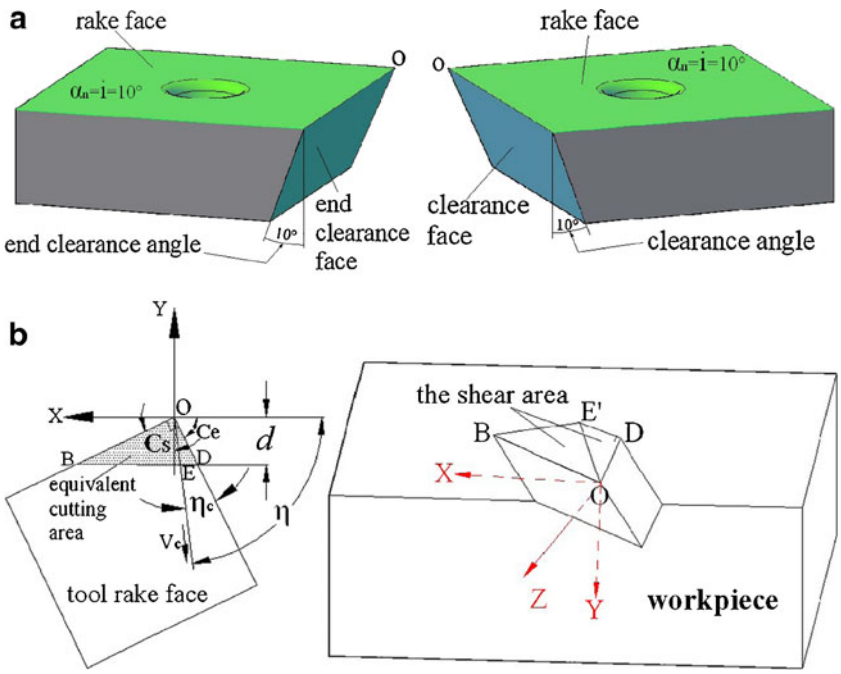

Fig. 5 Geometry (**a**) and the defined coordinate system (**b**) for the sharp point tool with zero inclination angle i and normal rake angle α_n, 10° of the clearance angle and the end clearance angle and 90° of the tool tip angle

$$\mathbf{OE}' = \frac{d}{\sin(\eta_C + Cs)} \cdot \begin{pmatrix} -\cos(\eta_C + Cs) \\ -\sin(\eta_C + Cs) \\ -\frac{V}{V_C} \end{pmatrix}$$

$$\mathrm{RATIO} = \frac{\mathrm{OB}}{\mathrm{OD}} = \frac{d/\cos Cs}{d/\sin Cs} = \tan C_S.$$

The value of RATIO can be expressed in terms of the variable C_S as:

The shear area of the triangular shear plane OBE′ can be calculated as:

$$S_{\Delta \mathrm{OBE}'} = 1/2^{*}|\mathbf{OB} \times \mathbf{OE}'| = \frac{1}{2} \cdot \frac{d}{\sin C_S} \cdot \frac{d}{\cos C_S} \cdot \left(\frac{1}{\cos \eta_c + \sin \eta_c / \mathrm{RATIO}} \cdot \sqrt{\left(\frac{1}{\tan \phi_e}\right)^2 + \cos^2 \eta_c} \right)$$
$$= A \cdot \left(\frac{1}{\cos \eta_c + \sin \eta_c / \mathrm{RATIO}} \cdot \sqrt{\left(\frac{1}{\tan \phi_e}\right)^2 + \cos^2 \eta_c} \right)$$

and the shear area of the triangular shear plane ODE′ can be calculated as:

$$S_{\Delta \mathrm{ODE}'} = 1/2^{*}|\mathbf{OD} \times \mathbf{OE}'| = A \cdot \left(\frac{1}{\cos \eta_c \cdot \mathrm{RATIO} + \sin \eta_c} \cdot \sqrt{\left(\frac{1}{\tan \phi_e}\right)^2 + \sin^2 \eta_c} \right)$$

So the total shear area A_S is the sum of the areas of the two triangular shear planes OBE′ and ODE′ and the shear energy W_S can be expressed as $W_S = \tau_S A_S V_S$.

2.3 The friction area calculation and the transformed expression of cutting power equilibrium

We assume that ΔL is an arbitrary line along the cutting edge with infinitesimal length and is the thickness of a slice of the effect cutting plane formed by V, V_S, and V_C as shown in Fig. 6.

For the slice of the effect cutting plane, the shear force f_S can be expressed as:

$$f_S = \tau_S \cdot l_S \cdot \Delta L.$$

l_S is the shear length of the slice of the effect cutting plane.

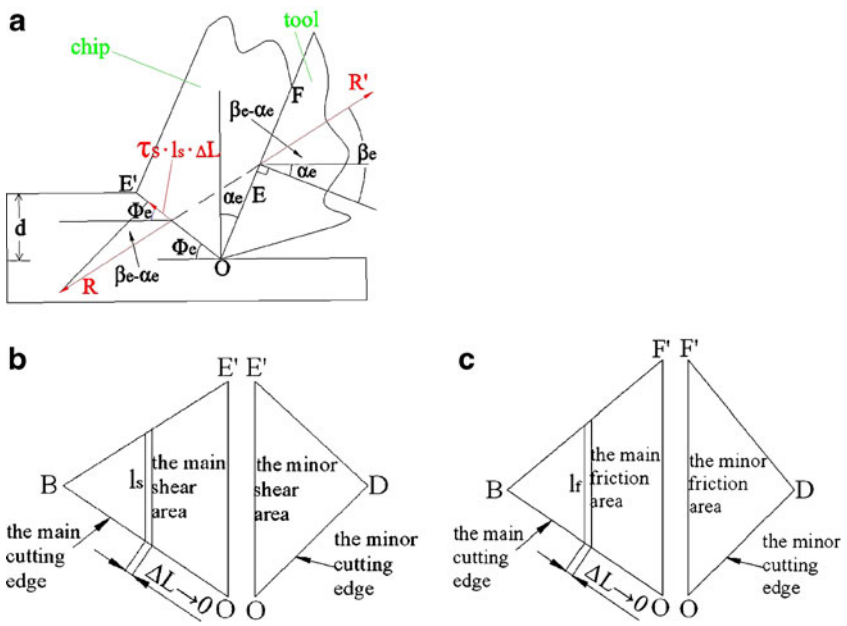

Fig. 6 Geometrical relations on the effect plane (**a**), the main and minor shear area (**b**), the main and minor friction area (**c**), and ΔL with infinitesimal length along the cutting edge

Usui et al. [11, 12] obtained the friction force f on the rake face:

$$f = R' \cdot \sin\beta_e = R \cdot \sin\beta_e = \frac{f_S}{\cos(\phi_e + \beta_e - \alpha_e)} \cdot \sin\beta_e \quad (3)$$
$$= \frac{\tau_S \cdot l_S \cdot \Delta L}{\cos(\phi_e + \beta_e - \alpha_e)} \cdot \sin\beta_e$$

R' is the reaction force of the resultant force acting on the rake face of the tool.

The friction force on the rake face can also be expressed as:

$$f = \tau_S \cdot l_f \Delta L \quad (4)$$

l_f is the friction length of the slice of the effect cutting plane.

We can obtain the relation between the shear length l_S and the friction length l_f from Eqs. 3 and 4:

$$l_f = \frac{\sin\beta_e}{\cos(\phi_e + \beta_e - \alpha_e)} \cdot l_S$$

So the friction length OF (L_f) corresponding to the common line OE′ (L_S) of the shear planes on the rake face of tool can be expressed as: $L_f = \frac{\sin\beta_e}{\cos(\phi_e+\beta_e-\alpha_e)} \cdot L_S$

The total friction area can be obtained by summing up the contact areas corresponding to the different regions of the shear planes. The total friction surface area is divided by OF into two areas ΔOBF and ΔODF which can be calculated with the same method of the shear areas calculation. The expression of the vector **OF** can be calculated as:

$$\mathrm{OF} = \frac{\sin\beta_e}{\cos(\phi_e+\beta_e-\alpha_e)} \cdot \frac{d\cdot\sqrt{1+\cot^2\phi_e}}{\sin(\eta_C+Cs)} \cdot \begin{pmatrix} -\cos(\eta_C + Cs) \\ -\sin(\eta_C + Cs) \\ 0 \end{pmatrix} = \frac{\sin\beta_e}{\cos(\phi_e+\beta_e)} \cdot \frac{d\cdot\sqrt{1+\cot^2\phi_e}}{\sin(\eta_C+Cs)} \cdot \begin{pmatrix} -\cos(\eta_C + Cs) \\ -\sin(\eta_C + Cs) \\ 0 \end{pmatrix}$$

The total friction area A_f can be computed as:

$$A_f = 1/2^*|\mathrm{OF} \times \mathrm{OB}| + 1/2^*|\mathrm{OF} \times \mathrm{OD}| = A \cdot \begin{pmatrix} \frac{1}{\cos\eta_c + \sin\eta_c/\mathrm{RATIO}} \cdot \sqrt{\left(\frac{\cos\eta_c}{\tan\phi_e}\right)^2 + \cos^2\eta_c} \cdot \frac{\sin\beta_e}{\cos(\phi_e+\beta_e)} + \\ \frac{1}{\cos\eta_c \cdot \mathrm{RATIO} + \sin\eta_c} \cdot \sqrt{\left(\frac{\sin\eta_c}{\tan\phi_e}\right)^2 + \sin^2\eta_c} \cdot \frac{\sin\beta_e}{\cos(\phi_e+\beta_e)} \end{pmatrix}$$

In this research, an ideal rigid plastic workpiece material with uniform distribution of the normal stress and sticking friction along the tool–chip interface is presumed to obtain the following estimate of friction angle β [24]:

$$\tan\beta = \frac{1}{1 + \frac{\pi}{2} - 2\alpha}$$

So the equivalent friction angle β_e can be calculated as:

$$\beta_e = \tan^{-1}\left(\frac{1}{1 + \frac{\pi}{2} - 2\alpha_e}\right) = 21.255^\circ$$

The friction force calculated by resolving the resultant cutting force along the tool rake face should be equal to the tool–chip interface area multiplied by the shear strength [14].

The shearing power W_S and the friction power W_f can be calculated as the expressions of

$$W_S = \tau_S A_S V_S = \tau_S \cdot A \cdot \begin{pmatrix} \frac{1}{\cos\eta_c + \sin\eta_c/\mathrm{RATIO}} \cdot \sqrt{\left(\frac{1}{\tan\phi_e}\right)^2 + \cos^2\eta_c} + \\ \frac{1}{\cos\eta_c \cdot \mathrm{RATIO} + \sin\eta_c} \cdot \sqrt{\left(\frac{1}{\tan\phi_e}\right)^2 + \sin^2\eta_c} \end{pmatrix} \frac{V}{\cos\phi_e}$$

and

$$W_f = \tau_S A_f V_C = \tau_S \cdot A \cdot \left(\begin{array}{l} \dfrac{1}{\cos\eta_c + \sin\eta_c/\mathrm{RATIO}} \cdot \sqrt{\left(\dfrac{\cos\eta_c}{\tan\phi_e}\right)^2 + \cos^2\eta_c} \cdot \dfrac{\sin\beta_e}{\cos(\phi_e+\beta_e)} + \\ \dfrac{1}{\cos\eta_c \cdot \mathrm{RATIO} + \sin\eta_c} \cdot \sqrt{\left(\dfrac{\sin\eta_c}{\tan\phi_e}\right)^2 + \sin^2\eta_c} \cdot \dfrac{\sin\beta_e}{\cos(\phi_e+\beta_e)} \end{array} \right) \cdot V\tan\phi_e,$$

respectively where A is the equivalent cutting area with a constant value and τ_S is the maximum shear stress. We substitute into cutting power equilibrium equation $V \cdot F = W_S + W_f$ [11, 12] with the expressions of the shearing power W_S and the friction power W_f to get the transformed expression of cutting power equilibrium of which the simplified format is expressed as:

$$\frac{F}{A\cdot\tau_S} = \left(\begin{array}{l} \dfrac{1}{\cos\eta_c + \sin\eta_c/\mathrm{RATIO}} \cdot \sqrt{\left(\dfrac{1}{\tan\phi_e}\right)^2 + \cos^2\eta_c} \\ + \dfrac{1}{\cos\eta_c \cdot \mathrm{RATIO} + \sin\eta_c} \cdot \sqrt{\left(\dfrac{1}{\tan\phi_e}\right)^2 + \sin^2\eta_c} \end{array} \right) \cdot \frac{1}{\cos\phi_e}$$

$$+ \left(\begin{array}{l} \dfrac{1}{\cos\eta_c + \sin\eta_c/\mathrm{RATIO}} \cdot \sqrt{\left(\dfrac{\cos\eta_c}{\tan\phi_e}\right)^2 + \cos^2\eta_c} \\ + \dfrac{1}{\cos\eta_c \cdot \mathrm{RATIO} + \sin\eta_c} \cdot \sqrt{\left(\dfrac{\sin\eta_c}{\tan\phi_e}\right)^2 + \sin^2\eta_c} \end{array} \right) \cdot \frac{\tan\phi_e \cdot \sin 21.255^\circ}{\cos(\phi_e + 21.255^\circ)} \quad (5)$$

Equation 5 can be a model to predict the chip flow angle η_c corresponding to specific value of RATIO with given cutting parameters such as equivalent cutting area A, the principal cutting force F and the equivalent shear angle Φ_e.

3 Model details

According to the theory of maximum shear stress [25], the maximum shear stress τ_S of the workpiece material can be calculated as $\tau_S = \sigma_S/2$ where σ_S is the yield stress of the workpiece material.

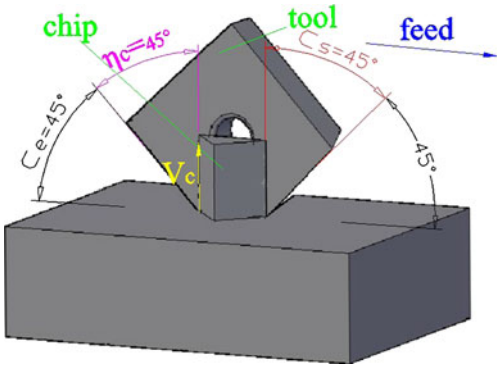

Fig. 7 Symmetric cutting with |OB|=|OD| and $C_S = C_e = 45°$

In literature [16], it is intuitively expected that the chip would flow normal to the feed direction for the cutting case with zero rake and inclination angle and the sum of the two cutting edge angles equal to 90°, which is confirmed by the predictions of the upper-bound model. In this study, we can deduce that the chip flow direction is parallel to the line about which the main and the minor cutting edges are symmetrical for the case of RATIO equal to 1. That is, the chip flow angle η_c equals 45° when the values of the main and the minor cutting edge angles (C_S and C_e) are all equal to 45°. This special cutting case can be called 'symmetric cutting' shown in Fig. 7.

With the experimental result of the main cutting force F and 45° of the chip flow angle η_c, we can get the value of the equivalent shear angle Φ_e according to Eq. 5 under the symmetric cutting condition with specific equivalent cutting area A. For asymmetric cutting conditions with the same equivalent cutting area A and various values of RATIO ranging from 1.2 to 10, the transformed cutting power equilibrium expression of Eq. 5 is substituted into with the calculated values of the equivalent shear angle Φ_e, the maximum shear stress τ_S, and the principal cutting force F experimentally measured corresponding to respective values of RATIO to obtain the different values of the chip flow angle η_c and study the effect of RATIO on the chip flow angle η_c. Figure 8 shows the procedure of the chip flow angle η_c calculation for the model expressed as the transformed cutting power equilibrium equation on the basis of the constant equivalent cutting area A.

The practical applications envisaged usually allow a tolerance for reasonable approximations, and the most likely approximations for this prediction model are the following:

1. The maximum shear stress τ_S on the shear plane may be assumed constant for one tool/workpiece pair over a reasonable range of cutting conditions and tool geometry [20].
2. The equivalent shear angle Φ_e corresponding to different values of RATIO is assumed to be constant

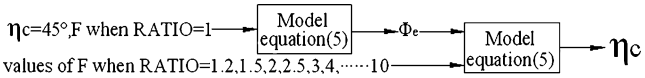

Fig. 8 Procedure of the chip flow angle η_c calculation of the model

Table 1 Simulation parameters

Surface speed (m/min)		50, 80, 120
Feed rate (mm/rev)		6, 8, 10
Tool–workpiece interface	Shear friction factor	0.6
	Heat transfer coefficient (N/s/mm/C)	45
Tool material		Cemented carbide
Workpiece material		AISI-1045(machining)
Workpiece type		Plastic
Relative mesh size of tool		40,000
Relative mesh size of workpiece		80,000
Simulation steps		500
The equivalent cutting area (mm^2)		0.9

based on the same equivalent cutting area A under specific vee groove turning conditions.

4 FEM simulation (work) for measurement of the chip flow angle η_c

FE simulations for 3-D oblique cutting were carried out on a series of cutting conditions with different values of RATIO to study the effects of RATIO on the chip flow angle η_c using the implicit dynamic analysis software 3-D DEFORM. Because machining is an extremely dynamic event with considerable changes in geometry, it is important to improve the mesh aspect by adopting an adaptive remeshing technique embedded in 3-D DEFORM. A series of cutting situations with the constant equivalent cutting area A and different values of RATIO ranging from 1.2 to 10 were considered in the FEM work. Simulation parameters are listed in Table 1.

The motion of the chip can be observed in the DEFORM-3D post-processor, and the chip flow angles corresponding to different values of RATIO are measured normal to the plane of the rake face of the tool shown in Fig. 9.

5 Experimental procedures

The experiments were conducted on a TK36 CNC lathe under dry condition. The workpiece material used in the experiments was AISI1045 steel (C 0.45%, Si 0.30%, Mn 0.60%, Cr 0.15%, Ni 0.20%, and S 0.02%), and the workpiece was held in a collet on the spindle. A tungsten carbide finishing tool conforming to the geometry of the sharp corner tool previously mentioned was used in the test. As shown in Fig. 10b, c, the tool was fixed in the three-axis turning dynamometer, and the turning dynamometer was positioned perpendicularly to the feed direction and directly mounted to the lathe. Before fixing the tool in the turning dynamometer, as shown in Fig. 10a, the tool position was adjusted by changing the main cutting edge angle C_S to satisfy the double-edge cutting condition with specific value of RATIO. The principal, vertical, and transverse force components were measured by the three-axis turning dynamometer during the oblique turning.

The filtered signals were sampled at 20 kHz, and the experimental data were processed and analyzed using MATLAB software. The Taguchi method is a robust experimental design technique, which adopts a set of orthogonal arrays to investigate the effect of parameters on specific quality characteristics to decide the optimum

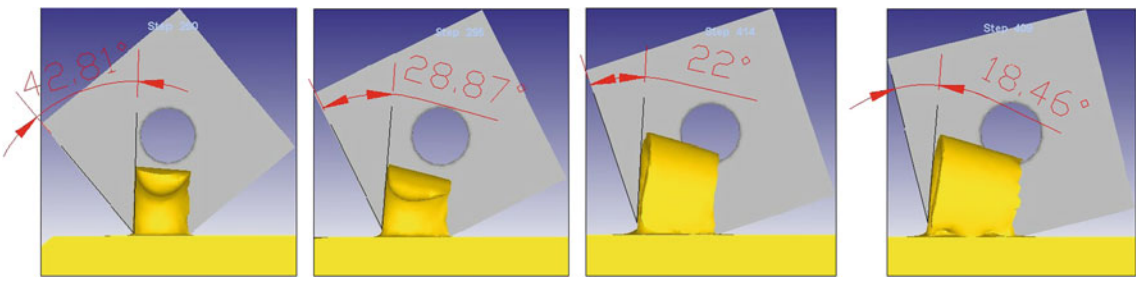

Fig. 9 Chip flow angle η_c measurement for various values of RATIO. **a** RATIO=1.2 for V=120 m/min, f=10 mm/rev, A=0.9 mm^2; **b** RATIO=2 for V=80 m/min, f=6 mm/rev, A=0.9 mm^2; **c** RATIO=3 for V=50 m/min, f=8 mm/rev, A=0.9 mm^2; **d** RATIO=4 for V=120 m/min, f=10 mm/rev, A=0.9 mm^2

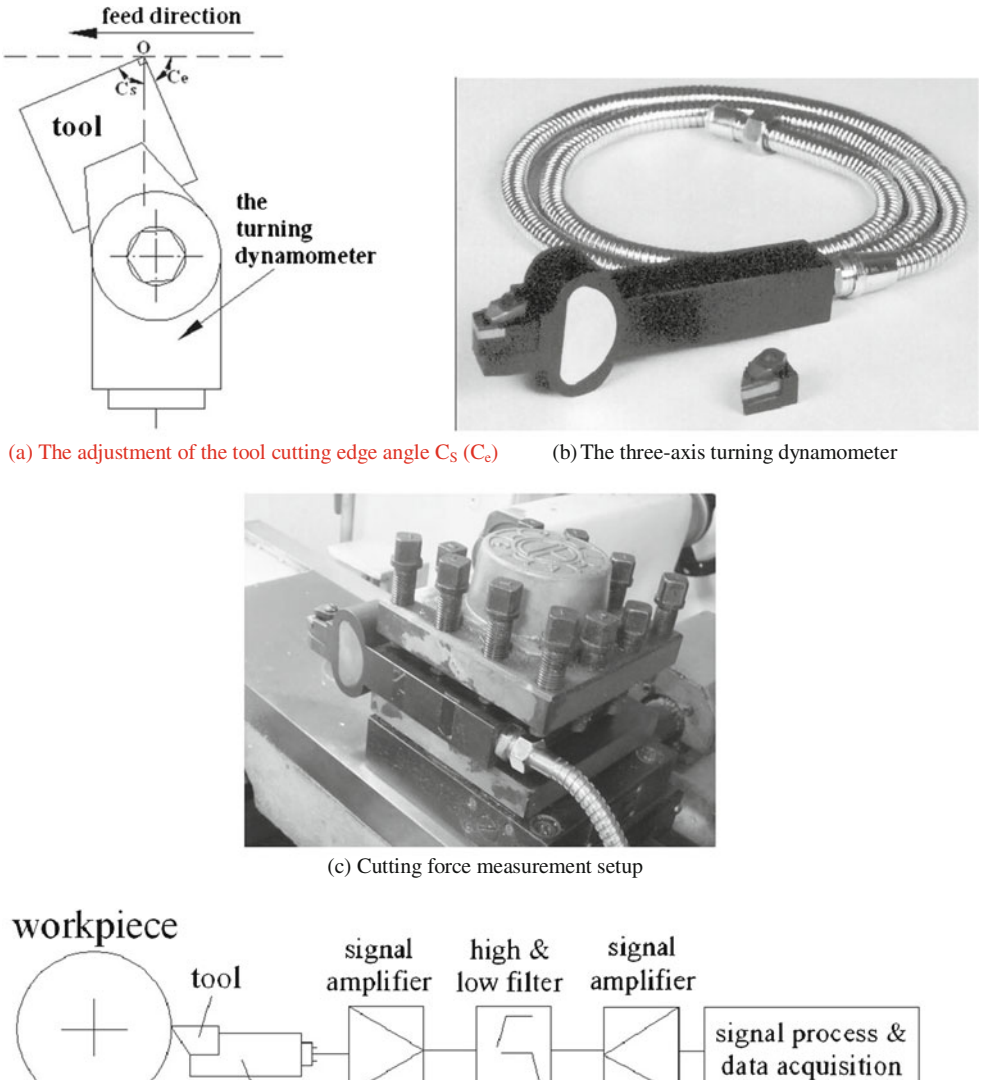

(a) The adjustment of the tool cutting edge angle C_S (C_e)

(b) The three-axis turning dynamometer

(c) Cutting force measurement setup

(d) Scheme of cutting force acquisition

Fig. 10 Cutting force measurement setup and procedure

parameter combination. Therefore, the orthogonal array has been widely applied in industries [26–28]. In our study, selections of cutting parameters for each level are shown in Table 2, and three levels of the machining parameters were selected. An L_9 orthogonal array table [29] is used to specify the experiments. This array table has three columns and nine rows, as shown in Table 3. Each combination of cutting experiments was conducted under different values of RATIO corresponding to their respective values of the main cutting edge angle C_S. For each combination of cutting experiments, the main cutting edge angle C_S and the depth of cut were changed according to the variation of RATIO. For example, as shown in Table 4, no. 7 of the cutting parameter combination of cutting experiment was conducted under different values of RATIO (or C_S).

Table 2 Cutting parameters and their levels

Symbol	Cutting parameters	Unit	Level 1	Level 2	Level 3
A	Cutting speed, V	m/min	50	80	120
B	Feed rate, f	mm/rev	6	8	10
C	Equivalent cutting area, A	mm^2	0.75	0.9	1.05

Table 3 Experimental layout using an L_9 orthogonal array

Number	Cutting parameter		
	A Cutting speed, V (m/min)	B Feed rate, f (mm/rev)	C Equivalent cutting area, A (mm^2)
1	50	6	0.75
2	50	8	0.9
3	50	10	1.05
4	80	6	0.9
5	80	8	1.05
6	80	10	0.75
7	120	6	1.05
8	120	8	0.75
9	120	10	0.9

5.1 The principal cutting force F measurement

The procedure of the principal cutting force acquisition is shown in Fig. 10c. The signals of the principal cutting force corresponding to different values of RATIO were obtained under the specific cutting case. As shown in Fig. 11, the signals of the principal cutting force were acquired under the cutting condition of 50 m/min of the cutting speed V, 8 mm/rev of the feed rate f, 0.9 mm^2 of the equivalent cutting area A, and 1:1 of the value of RATIO.

A mean value of the magnitude of the acquired signals is obtained as the principal cutting force F after statistical analysis. With this method, the other values of the principal cutting force F corresponding to other values of RATIO under the asymmetric cutting condition can be obtained.

Table 4 Experimental layout with respect to different values of RATIO under the cutting parameter combination 120 m/min of the cutting speed V, 6 mm/rev of the feed rate f, and 1.05 mm^2 of the equivalent cutting area A

Value of RATIO	C_S (deg)	Depth of cut (mm)
1	45	1.025
1.2	50.19	1.016
1.5	56.31	0.985
2	63.43	0.917
2.5	68.20	0.851
3	71.57	0.794
4	75.96	0.703
5	78.69	0.636
6	80.54	0.584
7	81.87	0.542
8	82.88	0.508
9	83.66	0.480
10	84.29	0.456

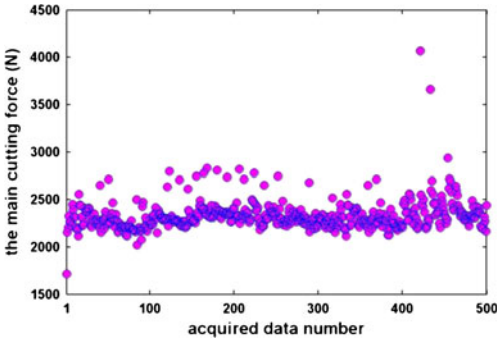

Fig. 11 Signals of the principal cutting force for the case of RATIO equal to 1

With the statistical result of the measured principal cutting force F, the equivalent shear angle Φ_e corresponding to the specific symmetric cutting condition with RATIO equal to 1 would be worked out according to Eq. 5. Subsequently, for the asymmetric cutting situations, the chip flow angle η_c corresponding to different values of RATIO ranging from 1.2 to 10 can be obtained with the calculated equivalent shear angle Φ_e and the statistical values of the principal cutting force F.

5.2 The chip flow angle η_c measurement

The measurements of the chip flow angle were made simultaneously using the techniques described in references [30]; the tool rake face of the cutting tool was painted with a paint which can resist high temperatures and create a strong adhesive layer with a substrate before machining. After every experiment, the trace which occurred with the abrasive effect of chip flowing on the rake face of the tool was observed using a workshop microscope, and its photograph was taken normal to the rake face of the tool by a camera setting on the workshop microscope. The file of the image of the chip trace was open using AutoCAD software and the chip flow angle was measured. Figure 12 shows the chip trace on the tool rake face and the chip flow angle η_c measured.

6 Results and discussion

With the experimental results of the principal cutting force F and the calculated value of the equivalent shear angle Φ_e, the predicted data of the chip flow angle η_c corresponding to different values of RATIO in Eq. 5 was generated by a computer program in MATLAB on the basis of the specific constant equivalent cutting area. In Fig. 13, the chip flow angle η_c corresponding to its value of RATIO shows excellent agreement with the experimental results, and FEM simulation results under the cutting conditions with

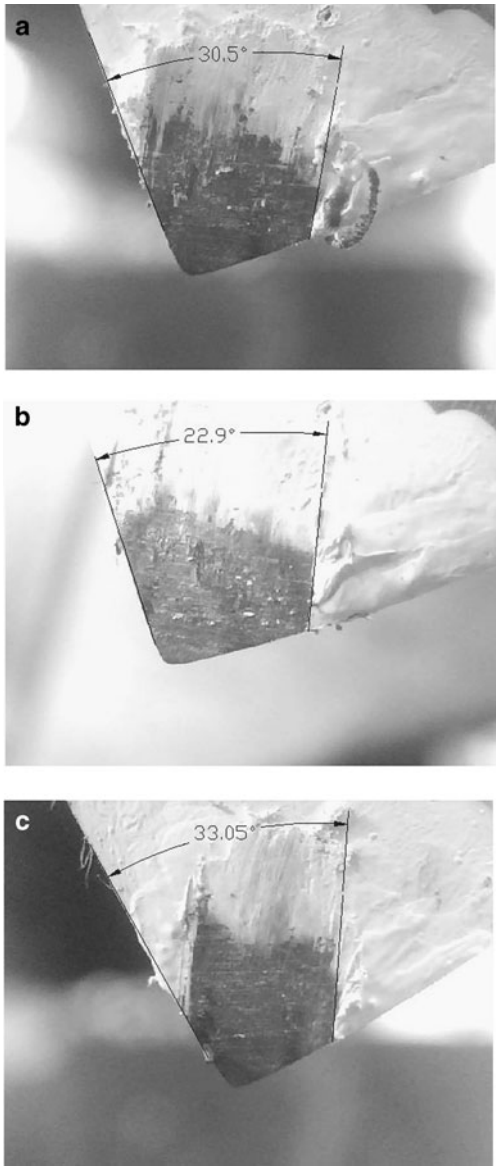

Fig. 12 Chip trace on the rake face for the cases of **a** RATIO=2, V=120 m/min, f=8 mm/rev, A=0.75 mm^2; **b** RATIO=3, V=80 m/min, f=8 mm/rev, A=1.05 mm^2; **c** RATIO=2, V=80 m/min, f=10 mm/rev, A=0.75 mm^2

0.9 mm^2 of the equivalent cutting area A; 6, 8, and 10 mm/rev of the feed rate f; and 50, 80, and 120 m/min of the cutting velocity V. A decrease in the chip flow angle η_c with an increase in the values of RATIO is presented provided that the equivalent cutting area A keeps constant. It is observed that RATIO shows a significant influence on the chip flow angle η_c.

Take Fig. 13a as an illustration, before RATIO comes to 4 (the main cutting edge angle C_S ranging from 50.194° to 75.964° with an increase of 25.77°, the chip flow angle η_c ranging from 42.798° to 16.713° with a drop of 26.085°, the lengths of the main and the minor cutting edges equal to 2.6832 and 0.6708 mm, respectively), the chip flow angle η_c shows a steep drop; when RATIO varies from 4 to 10 (the main cutting edge angle C_S increasing to 84.289° with an increase of 8.325°, the chip flow angle η_c decreasing to 7.1° with a drop of 9.613°, the lengths of the main and the minor cutting edges turning to be 4.243 and 0.4243 mm, respectively), the chip flow angle η_c shows a gentle drop.

The prediction results obtained under the cutting conditions mentioned in FEM work have a good correlation with the experimental results, and the ratio of the lengths of the two cutting edges play a significant role in the chip flow angle. It is suggested that with the increase in the values of RATIO, the length of the main cutting edge involved in cutting becomes larger to generate more chip while that of

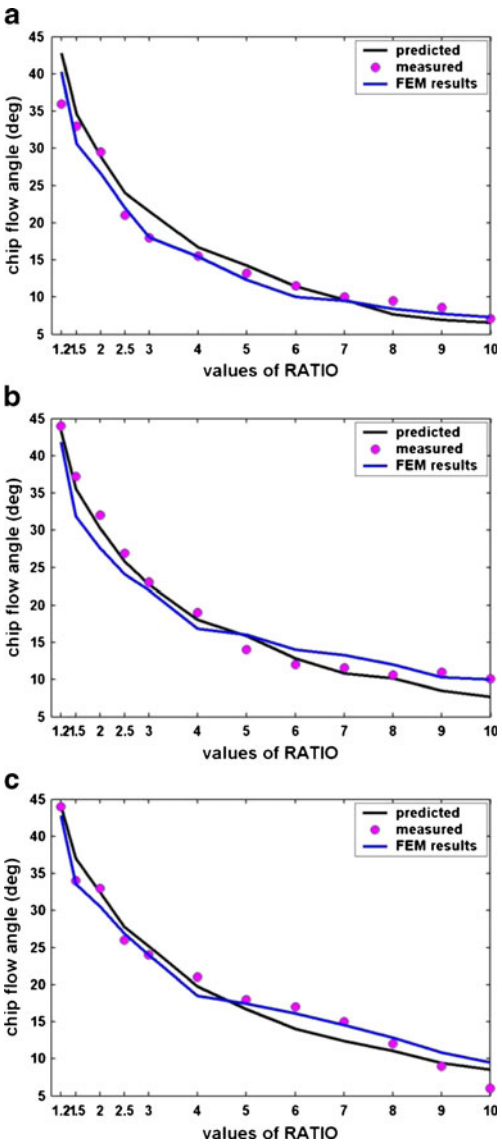

Fig. 13 Comparison of the chip flow angle measured experimentally and predicted by the derived cutting power equilibrium equation and FEM simulation while cutting with symmetric sharp corner tools for **a** A=0.9 mm^2, f=6 mm/rev, V=80 m/min; **b** A=0.9 mm^2, f=8 mm/rev, V=50 m/min; **c** A=0.9 mm^2, f=10 mm/rev, V=120 m/min

the minor cutting edge involved in cutting turns smaller to generate less chip, which makes the chip generated by the main cutting edge squeeze that generated by the minor cutting edge. As a result, the chip flow direction gets closer to the minor cutting edge and hence the chip flow angle η_c decreases. The chip flow motion can be regarded as the resultant motion of the chip generated by the main and the minor cutting edges, and the chip flow direction is determined by the separate directions of the chip generated by the two cutting edges as shown in Fig. 14. The total chip flows in the resultant direction in which the cutting power is in the minimum to satisfy the cutting power minimum principle [11, 12] for various cutting conditions.

Encouraged by the predicted results with good agreement with the experimental ones, the model expressed as Eq. 5 is extended to other cutting conditions listed in Table 3. In Fig. 15a~f, all the predicted results also agree well with the experimental results and have the same dropping trend. All the predicted and experimental results indicate that RATIO affects greatly the chip flow angle η_c, and the chip flow angle η_c decreases with the increase in the value of RATIO for the cutting case of the constant equivalent cutting area A. The drop trend of the chip flow angle η_c becomes slow when the value of RATIO increases to 4 under various cutting conditions listed in Table 3.

In addition, as can be seen from Fig. 15a–f, the results of Wen et al.'s model [18] of the chip flow angle prediction for sharp corner tools are compared with the results of the model expressed as Eq. 5 and the experimental results. The chip flow angle η_c predicted by the model expressed as Eq. 5 and the experimental results are all larger than that predicted by Wen et al.'s model [18] in which the revised coefficient k is chosen to be 0.9. The results predicted by the model of this study show smaller deviation from the experimental results than those of Wen's model [18]. It should be noticed that the curves of the chip flow angle η_c in Wen's model [18] stay the same shape regardless of the various cutting conditions as Table 3 listed. The Wen's model [18] of the chip flow angle prediction for the sharp corner tool was deduced only on the basis of the cutting situation that the feed rate f is not larger than the length of the equivalent cutting edge chord shown in Fig. 1 while in this study the cutting situations are all helical vee grooves turning with the larger feed rate f than the length of cutting chord BD shown in Fig. 2. So when the feed rate f exceeds the length of the equivalent cutting chord, the chip flow angle η_c corresponding to different values of RATIO predicted by Wen's model [18] just keeps its respective values invariant under various cutting conditions. Compared with the model expressed as Eq. 5, Wen's model [18] cannot satisfy the cutting case of helical vee grooves turning well.

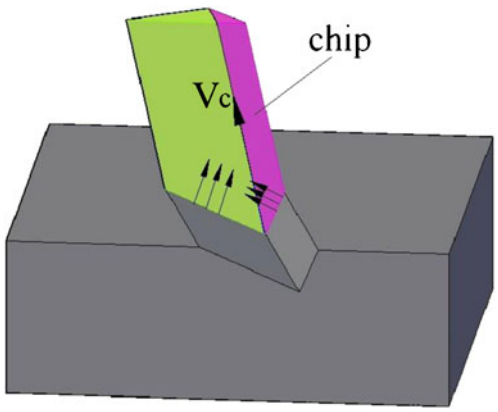

Fig. 14 Chip flow direction V_C comprised of chip flow directions generated by two cutting edges

The equivalent shear angle Φ_e varies with the cutting parameters such as the equivalent cutting area A, the feed rate f and the cutting speed V, which leads to the variation of the chip flow angle η_c according to Eq. 5. The chip flows in its direction to make the minimum cutting power and when the cutting situation changes, the chip motion will adjust its direction to generate new minimum cutting power. The chip flow angle is determined by the factors which affect the minimum cutting power, and the factors can be expressed as the variables in Eq. 5 such as the equivalent cutting area A, the principal cutting force F and RATIO.

7 Conclusion

The special cutting situation of helical vee grooves turning with the larger feed rate f than the length of the equivalent cutting chord BD leading to the two intersection points B and D all on the surface of the uncut workpiece shown in Fig. 2 is described to study the relation between RATIO and the chip flow angle η_c. Using the cutting power equilibrium expression of $W_S + W_f = V \cdot F$ [11, 12], a new chip flow angle prediction model expressed as the transformed expression of cutting power equilibrium is created, and the relation between the chip flow angle and the ratio of the main to the minor cutting edge length in engagement with the workpiece is studied based on the constant equivalent cutting area A for sharp corner tools. This study treats the chip flow direction as the result of the separate effects of the motions of the chip generated by the main and the minor cutting edges involved in cutting respectively. So when the value of RATIO changes, the resultant effects of the chip motions will make the chip adjust its flow direction to satisfy the minimum cutting energy principle [11, 12].

The predicted results in this study have a good correlation with the FEM simulation results and the experimental measurement under the cutting conditions 0.9 mm^2 of the constant cutting area A; 50, 80, and 120 m/min of the cutting

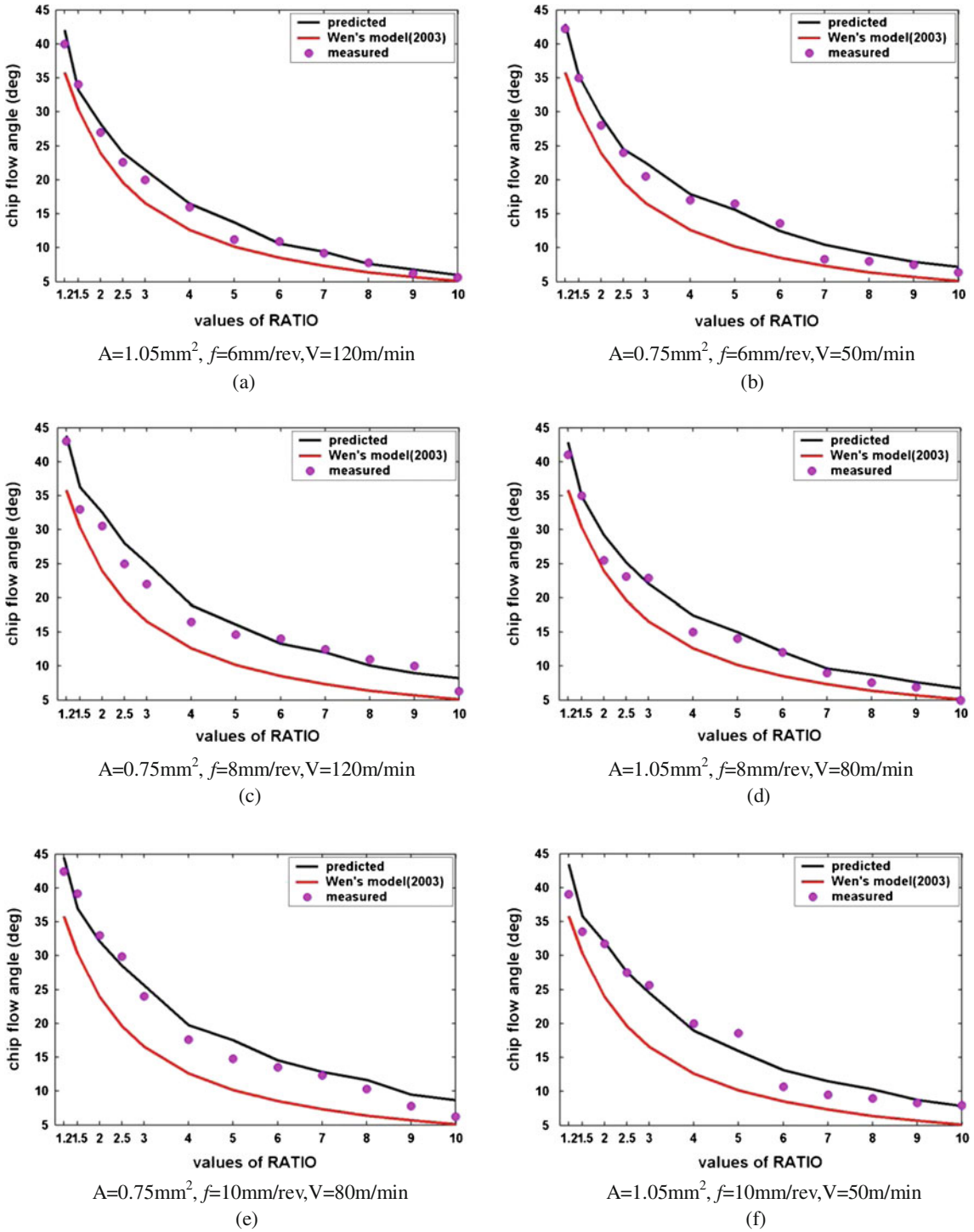

Fig. 15 Comparison of the chip flow angle versus values of RATIO predicted by this study and Wen's model [18] under various cutting conditions using sharp corner tools

speed V; and 6, 8, and 10 mm/rev of the feed rate f. Under various cutting conditions listed in Table 3, the results predicted by the model of this study show better agreement with the experimental results than those of Wen's model [18]. It is indicated that the chip flow angle decreases with the increase of the values of RATIO, and RATIO equal to 4 is the turning point before and after which the drop trend of the chip flow angle is different comparatively.

In this study, the principal cutting force F is obtained from experiments under specific cutting conditions to calculate the chip flow angle η_c, which improves the accuracy of the chip flow angle η_c prediction. That is

because chip formation involves a complicated deformation process; the chip flow angle η_c is significantly affected by the actual cutting situation and the principal cutting force F measured in experiments can reflect the effect of the actual cutting situation on the chip flow angle η_c according to Eq. 5. The factors which affect the chip flow angle η_c are directly embodied in the values of the principal cutting force F measured in the actual cutting situation. Substituting into Eq. 5 by the measured values of the principal cutting force F, the values of the chip flow angle η_c are calculated more accurately than just theoretical derivation without experimental data. The current prediction model of chip flow angle can be extended to study cutting cases with nose radius tools; the research on the relation between the chip flow angle and RATIO can be extended to study vee grooves shaping operation.

References

1. Jawahir IS, van Luttervelt CA (1993) Recent developments in chip control research and application. Ann CIRP 42:659–693
2. Van Luttervelt CA, Childs TH, Jawahir IS, Klocke F, Venuvinod PK (1998) Present situation and future trends in modeling of machining operations. Ann CIRP 47:587–626
3. Jawahir IS, Ghosh R, Fang XD, Li XP (1995) An investigation of the effects of chip flow on tool-wear in machining with complex grooved tools. Wear 184:145–154
4. Stabler GV (1951) The fundamentals geometry of cutting tools. Proc Inst Mech Eng 165:14–21
5. Stabler GV (1964) The chip flow law and its consequences. Proceedings of the 5th International Machine Tool Design and Research Conference. Pergamon Press, Oxford, pp 243–251
6. Armarego EJA, Brown RH (1969) The machining of metals. Prentice Hall, New Jersey
7. Colwell LV (1954) Predicting the angle of chip flow for single point cutting tools. Trans ASME 76(2):199–204
8. Hu RS, Mathew P, Oxley PLB, Young HT (1986) Allowing for end cutting edge effects in predicting forces in bar turning with oblique machining conditions. Proc Inst Mech Eng 200(part C):89–99
9. Okushima K, Minato K (1959) On the behavior of chip in steel cutting. Bull JSME 2(5):58–64
10. Young HT, Mathew P, Oxley PLB (1987) Allowing for nose radius effect in predicting the chip flow direction and cutting forces in bar turning. Proc Inst Mech Eng 201(C3):213–226
11. Usui E, Hirota A, Masuko M (1978) Analytical predictions of three dimensional cutting process: part 1 basic cutting model and energy approach. ASME J Eng Ind 100:222–228
12. Usui E, Hirota A (1978) Analytical prediction of three dimensional cutting process: part 2 chip formation and cutting force with conventional single point tool. ASME J Eng Ind 100:229–235
13. Shamoto E, Altintas Y (1999) Prediction of shear angle in cutting with maximum shear stress and minimum energy principles. J Manuf Sci Eng 121:399–407
14. Adibi-Sedeh AH, Madhavan V, Bahr B (2002) Upper bound analysis of oblique cutting with nose radius tools. Int J Mach Tools Manuf 42(9):1081–1094
15. Adibi-Sedeh AH, Madhavan V, Bahr B (2003) Upper bound analysis of oblique cutting: improved method of calculating the friction area. Int J Mach Tools Manuf 43:485–492
16. Adibi-Sedeh AH, Madhavan V (2004) Upper bound of turning using sharp corner tools. Mach Sci Technol 8:277–303
17. John SS, Albert JS, Lin JC (2002) An analytical finite element model for predicting three-dimensional tool forces and chip flow. Int J Mach Tools Manuf 42:723–731
18. Wen DH, Zheng L, Li ZZ, Hu RS (2003) An improved chip flow model considering cutting geometry variations based on the equivalent cutting edge method. Proc Inst Mech Eng B J Eng Manuf 217(12):1737–1745
19. Wen DH, Zheng L, Li ZZ, Hu RS (2004) On the prediction of chip flow angle in non-free oblique machining. Proc Inst Mech Eng B J Eng Manuf 218(10):1267–1278
20. Zou GP, Yellowley I, Seethaler RJ (2009) A new approach to the modeling of oblique cutting processes. Int J Mach Tools Manuf 49:701–707
21. Dogra AJS, Kapoor SG, Devor RE (2002) Mechanistic model for tapping process with emphasis on process faults and hole geometry. J Manuf Sci Eng 124:18–25
22. Suzuki T, Ariura Y, Umezaki Y (1993) Basic study on cutting forces in gear cutting: theory of cutting with two continuous symmetrical cutting edges. JSME Int J 36:543–549
23. Wang J (2001) Development of a chip flow model for turning operations. Int J Mach Tools Manuf 41:1265–1274
24. Seethaler RJ, Yellowley I (1997) An upper-bound cutting model for oblique cutting tools with a nose radius. Int J Mach Tools Manuf 37(2):119–134
25. Gere JM (2001) Mechanics of materials. Thomson Learning, Kentucky
26. Lan TC, Wang MY (2009) Competitive parameter optimization of multi-quality CNC turning. Int J Adv Manuf Technol 41:820–826
27. Mohan LV, Shunmugam MS (2006) An orthogonal array based optimization algorithm for computer-aided measurement of worm surface. Int J Adv Manuf Technol 30:434–443
28. Jeang A, Chang CL (2002) Combined robust parameter and tolerance design using orthogonal arrays. Int J Adv Manuf Technol 19:442–447
29. Lin CL, Lin JL, Ko TC (2002) Optimisation of the EDM process based on the orthogonal array with fuzzy logic and grey relational analysis method. Int J Adv Manuf Technol 19:271–277
30. Murat K, Mirigul A, Erhan A (2007) Prediction of chip flow angle in orthogonal turning of mild steel by neural network approach. Int J Adv Manuf Technol 33:251–259
31. Bradley HJ, Thomas AD (2001) Investigation of the direction of chip motion in diamond turning. Precis Eng 25(2):155–164